Effects of Dipping Layers on TEM 1D-Inversion

S. Hölz, T. Hiller & H. Burkhardt
Angew. Geowissenschaften, FR Geophysik
TU Berlin

Introduction

In the interpretation of central-loop or coincident-loop TEM-measurements, 1D inversion-codes are most commonly used for data evaluation. In the vicinity of 2D/3D structures, i.e. close to subvertical conductivity contrasts, 1D inversions of transients produce fictitious layers, which can lead to misinterpretations. Several authors have used 3D modeling-codes to investigate and describe the general effects, which can occur when using 1D inversions on 2D/3D data sets:

- Goldman et al. (1994) and Rabinovich (1995) use a finite difference (FD) algorithm, described in Tabarovsky et al. (1995), to calculate transient responses for the central-loop- and the long-offset-configuration (LOTEM). They investigate the transient response of a rotational symmetric body in a layered host for arbitrary receiver and transmitter locations. Because of the rotational symmetry, model bodies are confined in x- and y-direction and the resulting overall model can therefore considered to be 3D (fig. 1, top). The authors use a 1D block-inversion-code to interpret the 3D transients.
- Toft (2001) uses the 3D code of Árnason (1999) to calculate the transient response of buried valley structures (fig. 1, middle) for a central-loop and a separate-loop configuration. The geometry of models in his work is 2D, i.e. resistivities do not change in y-direction. The calculated 2.5D transients are inverted using a 1D smooth-inversion-code. Some results of his thesis can be found in Danielsen et al. (2003).

In our study we first test the feasibility of the 3D code of Árnason (1999) to calculate transients for the coincident-loop configuration, which has been used in most of our measurements. Transients calculated with the 3D code are compared for a variety of grids with 1D-transients of homogeneous and layered halfspaces.
We then further simplify the models of Toft (2001), which now only include a dipping layer with infinite depth extent (fig. 1, bottom). We gradually change the angle of inclination for the dipping layer to study general effects of 1D inversion of 2.5D data sets and to see, if the true angle of inclination can be recovered.

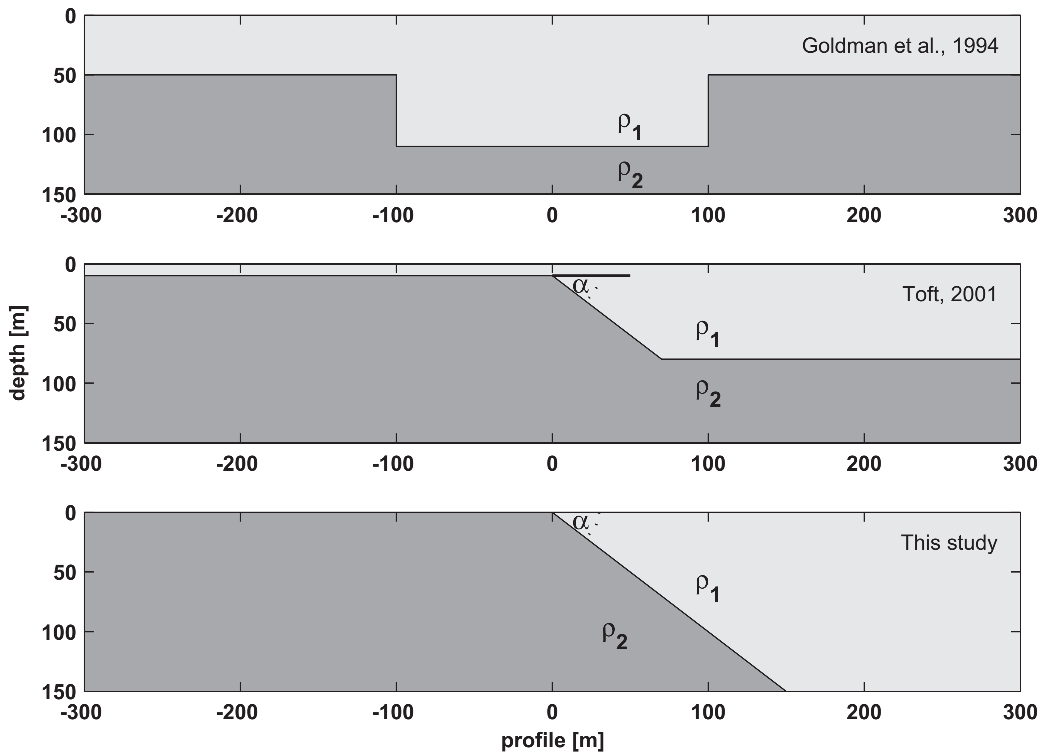

Fig. 1: Basic model types
Top: Submerged valley consisting of a rotational symmetric body in a layered host (Goldman et al., 1994).
Middle: Half of a submerged valley (Toft, 2001). The dip α is varied between 11.25°-90°.
Bottom: Simplified model for this study. The dip α is varied between 10°-90°.

Numerical Testing

General

In this model study the 3D modeling code TEMDDD (Árnason, 1999) is used to calculate transient responses over 2D models (fig. 1, bottom). The program uses the SLDM (Spectral Lanczos Decomposition Method (Druskin & Knizhnerman, 1988)) to solve the finite difference formulation of the transient electromagnetic problem in the time domain. A concise description of the program and suggestions for the choice of input parameters (i.e. discretization parameters and size of generalized derivative matrix) can be found in Weidelt (2000). In numerical testing the input parameters to TEMDDD are chosen and adjusted according to the following constraints:

- coincident-loop configuration, 100 x 100 m²
- earliest time in transient: 30µs
- minimum voltage of transient: 10^{-2} nV/Am²
- resistivity range of models: 1-1000 Ωm
- maximum error with respect to transient of homogenous halfspace: <1%
- constant grid spacing in xy-direction for cells inside the loop
- outward increasing grid spacing in xy-direction (Δxy) outside the loop

(1) $$\Delta xy_{i+1} = f_{xy} \cdot \Delta xy_i \qquad f_{xy} > 1$$

- downward increasing grid spacing in z-direction (Δz)

(2) $$\Delta z_{i+1} = f_z \cdot \Delta z_i \qquad f_z > 1$$

The transient response for the coincident-loop configuration is calculated by numerical integration of the inloop-responses for all cells located inside the loop. The minimum time for testing is chosen corresponding to the earliest analyzable time for real measurement systems, which is determined by the minimum ramp time of ~30µs for a 100 x 100 m² loop. In contrast to Toft (2001), who determines the input parameters to TEMDDD for a fixed time interval, we choose a variable maximum time limit (t_{max}) determined by the resolution of the measurement system, which in our case is estimated as minimum normalized voltage of ~10^{-2} nV/Am² for a 100 x 100m² loop.

The number of required time steps N_t (resp. dimension of the generalized derivative matrix for the SLDM), which controls the accuracy of the solution at late times, is coupled to the Courant-Friedrichs-Lewy criterion and has the general form:

(3) $$N_t \cong \frac{f}{\Delta_{min}} \cdot \sqrt{\frac{t_{max}}{\mu_0 \sigma_{min}}}$$

N_t greatly influences computational time and has to be chosen with respect to the required accuracy of solution. Estimates according to several publications are summarized in tab. 1.

Homogeneous Halfspace & Layered Halfspace

In a first step transients are calculated with TEMDDD for homogeneous halfspaces (1-1000 Ωm) and compared to the transients calculated with a 1D code. The input parameters to TEMDDD are successively adjusted to find an appropriate discretization for each halfspace.

Resistivity of Halfspace	t_{max} [ms]	Oristaglio & Hohmann (1984)	Adhidjaja & Hohmann (1989)	Wang & Hohmann (1993)	Weidelt (2000)
		$f = 2$	$f = \sqrt{6}$	$f = \frac{\sqrt{6}}{\alpha}$ $\alpha = 0.1 - 0.2$	$f = \frac{1}{\alpha}$ $\alpha = 0.05 - 0.1$
1 Ωm	191	156	190	953-1905	778-1555
10 Ωm	48	247	302	1512-3025	1235-2470
100 Ωm	12	391	479	2394-4787	1954-3909
1000 Ωm	3	618	757	3785-7569	3090-6180

Tab. 1: Number of required time steps (N_t) according to (3) with factors f as specified by different authors. A minimum grid spacing of 5m is assumed. The maximum time t_{max} is determined by the resolution of the measurements system ($V_{min} \sim 10^{-2}$nV/Am^2).

Halfspace	N_{xy}	f_{xy}	N_z	f_z	N_t	Dim [m]
1 Ωm	42	1.17	24	1.15	1000	3112x980
10 Ωm	48	1.17	27	1.15	1500	5137x1504
100 Ωm	52	1.17	29	1.15	1800	7184x2000
1000 Ωm	56	1.17	32	1.15	3000	9900x3055

Tab. 2: Final optimized parameters of input models to TEMDDD for homogeneous halfspaces. N_{xy} and N_z refer to the number of grid cells in xy- resp. z-direction.

After some testing, the factors controlling the downward and outward increasing grid dimensions are fixed to 1.15 (f_z, see (2)) and 1.17 (f_{xy}, see (1)). The 100x100m^2-loop is discretizised with 14x14 cells to stabilize the integration for the calculation of the coincident-loop response. To keep model discretizations for input models of different half spaces comparable, larger grids are constructed by simply adding additional cells to the outer bounds of the model. The dimensions of the added cells are chosen according to (1) and (2).
When using grids as summarized in tab. 2 the error, as compared to the 1D code, is generally <1% for all relevant times (tab. 1). Only for the lowest resistivities of 1Ωm and times <300µs the relative error exceeds 1% and reaches values of up to 12%. This behavior for low resistivities and early times is due to the high frequency cut off caused by the finite discretization (Árnason, 2000) and can only be circumvented by introducing a refined grid.
For a test with three-layered halfspaces (100Ωm/10Ωm/100Ωm and 10Ωm/100Ωm/10Ωm) we use the discretization parameters found for the 100Ωm halfspace (tab. 2) and vary the interface depths. The comparison with the according transients calculated with the 1D code is still

generally <1%. Only for very early and very late times the relative error exceeds 1% and can reach values of up to 5% for a few time steps. Further comparisons of TEMDDD with other 3D TEM-codes has not been performed in this study, but can be found in Toft (2001).

Modeling of Dipping Layers

We use the discretization parameters for the 100Ωm halfspace (tab. 1) to construct dipping layer models as depicted in fig. 1, bottom. The resistivity contrast between the upper and lower layer is set to 100Ωm:10Ωm respectively 10Ωm:100Ωm and the angle of inclination is varied between 10°-90°. For cells intersected by the dipping layer (fig. 2), an average conductivity value is calculated weighted proportionally to the intersected areas to facilitate the construction of models and to minimize errors caused by the discretization:

$$\sigma_{cell} = \frac{\sigma_1 A_1 + \sigma_2 A_2}{A_{cell}} \tag{4}$$

Transients are calculated for stations every 100m, i.e. the coincident loop configuration respectively the discretization grid is shifted along the profile. The resulting transients are then inverted using a 1D block inversion code. The number of layers used for inversion is varied according to the resulting rms-error. A maximum of three layers is sufficient to arrive at an rms-error <1.5% in the 1D inversion. Results are summarized in fig. 3.

With the resistor as top layer and small to moderate angles of inclination (fig. 3, left column, $\alpha \leq 30°$) the combination of 1D inversion results closely resemble the true models. A fictitious second layer of intermediate resistivity is produced by the 1D inversion above the dipping layer of the true model (white line). For larger angles of inclination ($\alpha \geq 45°$) additional

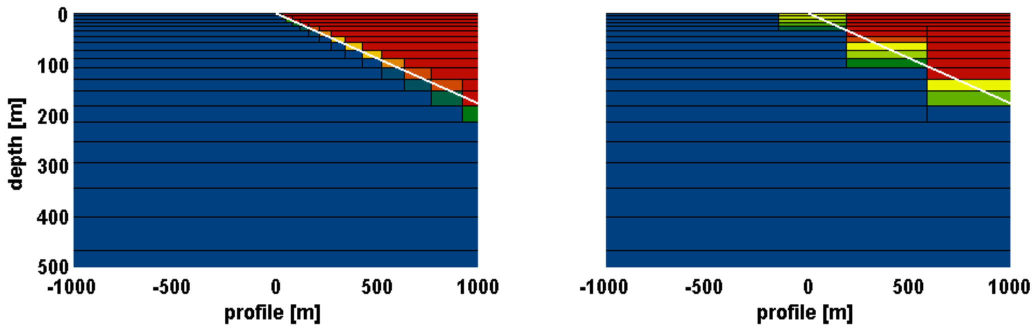

Fig. 2: Extract of example input models for TEMDDD with loops located at 0m (left) and -2000m (right). For cells intersected by the dipping layer (white line) an average conductivity is calculated (4). For the sake of clarity, cell boundaries are only displayed in x-direction for cells intersected by the dipping layer. For the color scale refer to fig. 3.

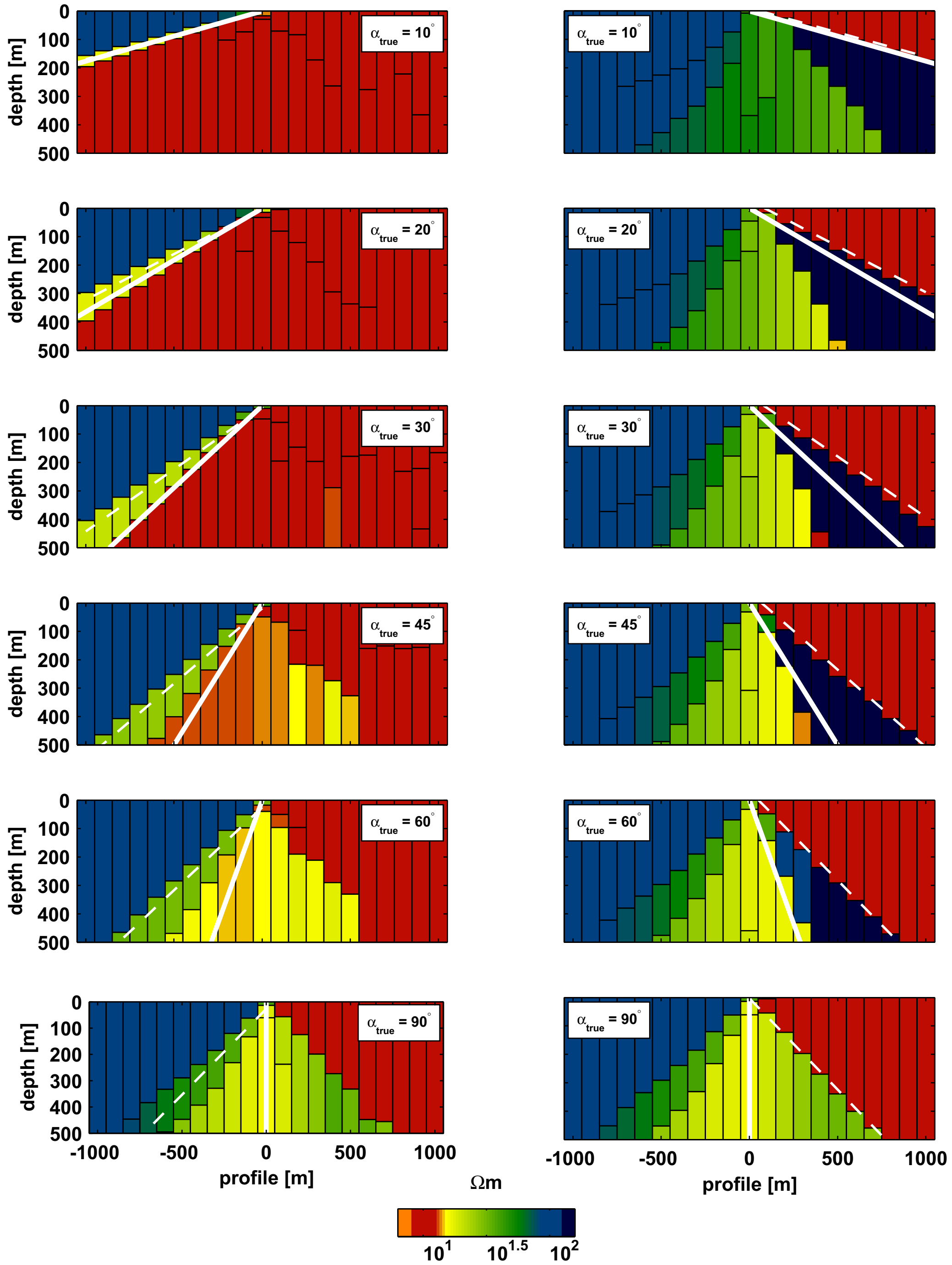

Fig. 3: Results for 1D block inversions of 2.5D transients calculated with TEMDDD (*left*: top layer is resistor (100Ωm); *right*: top layer is conductor (10Ωm)). All resistivities within 10% of the true resistivity are colored alike. At each station we chose the model with a minimum number of layers and acceptable rms (generally ≤1%). The true resp. apparent inclination of the dipping layers are represented by solid respectively dashed white lines. A model study with changed resistivity contrasts (s. text) leads to essentially the same geometry for the 1D inversion results.

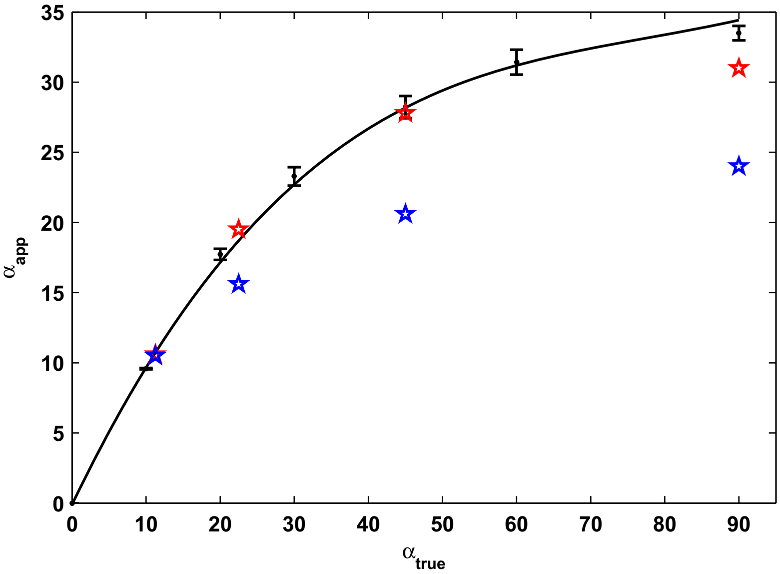

Fig. 4: Relationship between apparent and true angle of inclination (black) with a cubic polynomial fit (5). The apparent inclination refers to the white dashed line in fig. 3. Error bars represent the standard deviation of the apparent inclination for all models (resistivity contrasts: 10Ωm:17.8Ωm, 10Ωm:31.6Ωm, 10Ωm:56.2Ωm, 10Ωm:100Ωm and vice versa). Colored pentagrams depict results as estimated from Toft (2001). For further details see discussion.

fictitious anomalies are also introduced in the homogeneous parts of the true models (i.e. for x>0m). The anomalous regions have a pyramidal wedge shape.

With the conductor as top layer (fig. 3, right column) the anomalous pyramidal wedge is visible for all models, less pronounced for small angles of inclination. Below the dipping layer (i.e. for x>0m) the resistivity of the second layer is overestimated. A sensitivity analysis for the 1D inversion results shows that this parameter is poorly resolved.

For all models the first layer interface above the dipping layer underestimates the true angle of inclination. When comparing models with the same angle of inclination but swapped resistivity contrast (e.g. 100Ωm:10Ωm and 10Ωm:100Ωm, α=20°) it can be seen that the depth of this first layer interface for both model types is essentially equal. Additional testing with resistivity contrasts of 10Ωm:17.8Ωm, 10Ωm:31.6Ωm, and10Ωm:56.2Ωm (and vice versa) yield the same relation between the true angle of inclination and the depth of the first layer interface, which yields an "apparent inclination". In fig. 4 the relationship between true and apparent angle of inclination is shown for all resistivity contrasts. The small error bars demonstrate that the apparent inclinations for all resistivity contrasts referring to the same true inclination are similar.

Curve fitting can therefore be used to calculate the true inclination from the apparent inclination (and vice versa). Cubic polynomial fits yield (5). For steep angles of inclination (α_{true}>60°) the apparent inclination does not change significantly any more and the errors of the estimates increase. Estimates using (5) should therefore be restricted to inclinations of α_{true}≤60° respectively α_{app}≤30°.

$$\begin{aligned} \alpha_{app} &\approx 5.6(3)\cdot 10^{-5}\cdot \alpha_{true}^3 - 1.3(1)\cdot 10^{-2}\cdot \alpha_{true}^2 + 1.1\cdot \alpha_{true} - 0.1 \\ \alpha_{true} &\approx 2.7(2)\cdot 10^{-3}\cdot \alpha_{app}^3 - 7.5(1)\cdot 10^{-2}\cdot \alpha_{app}^2 + 1.6\cdot \alpha_{app} - 0.1 \end{aligned} \tag{5}$$

Discussion

Results for the 1D block inversions of 2.5D transients can be explained by the concept of "smoke rings" as introduced by Nabighian (1979). He shows that the diffusive current system induced by a loop into a homogeneous halfspace travels downward and outward away from the exciting loop with the maximum of the current system moving at an angle of approximately 30° with respect to the surface. This means that for a loop positioned above a dipping layer (fig. 3, x<0 for left column, x>0 for right column) the current system will, due to it’s outward propagation, always be influenced by the conductivity change, even for steep inclinations of the dipping layer. The same holds true for steep inclinations (α≥45°) above the homogeneous part of models (fig. 3, x>0 for left column, x<0 for right column). For small inclinations (α≤30°) and high resistivities in the homogeneous part of models (fig. 3, x<0 for right column), the maximum of the current system is shifted into the conductive top layer, due to the sensitivity of the TEM-method to conductors, which causes the 1D inversion to produce ficticious layers. For small inclinations (α≤30°) and high conductivities in the homogeneous part of models (fig. 3, x>0 for left column) the propagation of the current system is not significantly influenced by the resistive top layer and the 1D inversions thus reflect the homogeneous structure in this part of the model.

By visual comparison, the results in Toft (2001) – calculated for a slightly more complicated model type (fig. 1, middle), the central-loop configuration (40x40m^2), and inverted using a 1D smooth-inversion code – compare well to our study for the case of a conductive basement (red pentagrams in fig. 4), but show significant deviations for the case of a resistive basement (blue pentagrams in fig. 4). It remains unclear, if this deviation is caused by the use of the 1D smooth inversion code, which might exhibit a different sensitivity to the lower edge of a conductive structure, or if it is simply caused by the subjective visual inspections of the color plots in Toft

(2001). The studies of Goldman et al. (1994), and Rabinovich (1995) yield smaller apparent inclination for a true inclination of 90° (with respect to (5)), but rely on a considerably different, true 3D model type (fig. 1, top).

Conclusion

In this model study we examine the effects produced by the 1D block inversion of 2.5D transients, where the basic model type is a dipping layer with varying angles of inclination. The interpretation of the 1D results generally leads to an underestimation of the true inclination and introduces ficticious layers, which is in accordance with the studies of Goldman et al (1994), Rabinovich (1995), and Toft (2001).

We show that for moderate inclinations ($\alpha \leq 60°$) the true inclination can be estimated from the apparent inclination (→ (5)). Further modelling suggests that within the tested resistivity range the relationship between true and apparent inclination does not depend on the resistivity contrast.

Below the dipping layer an additional ficticious homogeneous dipping layer is introduced by the 1D inversion. Especially for the case of a resistive basement additional dipping layer interfaces are also introduced in the homogeneous part of the model. These artifacts contain no additional significant information and need to be excluded from interpretation.

Acknowledgement

We wish to thank Knútur Árnason for allowing us to use his 3D code TEMDDD. This model study has been inspired by the thesis of Toft (2001).

References

Árnason, K.: A Short Manual For The Program TEMDDD. 2000, 7p.

Árnason, K.: Consistent discretization of electromagnetic fields and transient modeling. *In* Oristaglio, M. Spies, B. & Cooper, M. (ed.): Three-Dimensional Electromagnetics. SEG, 1999, pp. 103-118.

Adhidjaja, J. & Hohmann, G.: A finite-difference algorithm for the transient electromagnetic response of a three-dimensional body. Geophysical Journal International, 1989, vol. 98, pp. 233-242.

Danielsen, J., Auken, E., Jorgensen, F., Sondergaard, V. & Sorensen, K.: The application of the transient electromagnetic method in hydrogeophysical surveys. Journal of Applied Geophysics, 2003, vol. 53, pp. 181-198.

Druskin, V. & Knizhnerman, L.: Spectral differential-difference method for numeric solution of three-dimensional nonstationary problems of electric prospecting. Izvestiya, Earth Physics, 1988, vol. 24, pp. 641-648.

Goldman, M., Tabarovsky, L. & Rabinovich, M.: On the influence of 3-D structures in the interpretation of transient electromagnetic sounding data. Geophysics, 1994, vol. 59, pp. 889-901.

Nabighian, M.: Quasi-static transient response of a conducting half-space: An approximate representation. Geophysics, 1979, vol. 44, pp. 1700-1705.

Oristaglio, M. & Hohmann, G.: Diffusion of electromagnetic fields into a two-dimensional earth: A finite-difference approach. Geophysics, 1984, vol. 49, pp. 870-894.

Rabinovich, M: Errors of 1-D interpretation of 3-D TDEM data in the application of mapping saltwater / freshwater contact. Journal of Applied Geophysics, 1995, vol. 34, pp. 23-34.

Tabarovsky, L., Goldman, M., Rabinovich, M. & Strack, K.: 2.5D-modeling in electromagnetic methods of geophysics. Journal of Applied Geophysics, 1995, vol. 35, pp. 261-284.

Toft, M.: Three-dimensional TEM modeling of nearsurface resistivity variations. MSc-thesis, University of Aarhus, Denmark, 2001.

Wang, T. & Hohmann, G.: A finite-difference, time-domain solution for three-dimensional electromagnetic modeling. Geophysics, 1993, vol. 58, pp. 797-809.

Weidelt, P.: Numerical modelling of transient-electromagnetic fields in three-dimensional conductors: A comparative study. Elektromagnetische Tiefenforschung, Kolloquiumsband zur Tagung in Altenberg, 2000, pp. 216-230.